

## Constraint on the post-Newtonian parameter $\gamma$ on galactic size scales

Adam S. Bolton,<sup>1,\*</sup> Saul Rappaport,<sup>2</sup> and Scott Burles<sup>2</sup>

<sup>1</sup>*Harvard-Smithsonian Center for Astrophysics, 60 Garden St., Cambridge, Massachusetts 02138 USA*

<sup>2</sup>*Department of Physics and Kavli Institute for Astrophysics and Space Research, Massachusetts Institute of Technology, 77 Massachusetts Ave., Cambridge, Massachusetts 02139 USA*

(Received 28 July 2006; published 8 September 2006)

We constrain the post-Newtonian gravity parameter  $\gamma$  on kiloparsec scales by comparing the masses of 15 elliptical lensing galaxies from the Sloan Lens ACS Survey as determined in two independent ways. The first method assumes only that Newtonian gravity is correct and is independent of  $\gamma$ , while the second uses gravitational lensing which depends on  $\gamma$ . More specifically, we combine Einstein radii and radial surface-brightness gradient measurements of the lens galaxies with empirical distributions for the mass concentration and velocity anisotropy of elliptical galaxies in the local universe to predict  $\gamma$ -dependent probability distributions for the lens-galaxy velocity dispersions. By comparing with observed velocity dispersions, we derive a maximum-likelihood value of  $\gamma = 0.98 \pm 0.07$  (68% confidence). This result is in excellent agreement with the prediction of general relativity that  $\gamma = 1$ , which has previously been verified to this accuracy only on solar-system length scales.

DOI: [10.1103/PhysRevD.74.061501](https://doi.org/10.1103/PhysRevD.74.061501)

PACS numbers: 04.25.Nx, 04.80.Cc

Gravitational lenses provide some of the most inspirational and thought-provoking images in astronomy. It is often said in the popular press that these represent a wonderful verification of Einstein's general theory of relativity (GR). In 1937, Zwicky [1] proposed that lensing by distant galaxies and clusters would furnish both a test of GR and a tool for the measurement of the lensing masses. Since the discovery of the first gravitational lenses, however, astronomers have emphasized the latter application over the former. In fact, gravitational lensing alone cannot simultaneously determine the masses of lenses and test the weak-field limit of the Schwarzschild metric which underlies the theory of lensing.

Since Eddington's original solar eclipse expedition of 1919, the Schwarzschild metric has been extensively probed in the weak-field limit within the solar system (e.g. [2]) and with binary radio pulsars (e.g. [3]). In all cases, however, the scales involved are of order light seconds. Most recently, the Cassini mission has determined the post-Newtonian parameter  $\gamma$  (e.g. [4,5]), described below, by directly measuring the Shapiro delay [6] as radio signals pass by the Sun in their travel from the spacecraft to the Earth, giving a measured value of  $\gamma = 1 + (2.1 \pm 2.3) \times 10^{-5}$  [2]. In this paper we set precise constraints on  $\gamma$  on galactic scale sizes of several kiloparsecs (1 pc  $\approx 3.1 \times 10^{18}$  cm): impact parameters  $\sim 10^{11}$  times larger than in Sun-grazing solar-system tests. We accomplish this by comparing the masses of relatively low-redshift ( $0.06 < z < 0.33$ ) galaxies as deduced from strong gravitational lensing with their masses as estimated from their stellar orbital dynamics. Since the former determination depends upon GR through the value of  $\gamma$ , whereas the latter depends only upon Newtonian gravity, the quantitative

agreement between the two methods can place a direct constraint upon  $\gamma$ . Our analysis constrains  $\gamma$  to have a value of  $0.98 \pm 0.07$  (68% confidence), in excellent agreement with the GR prediction of  $\gamma = 1$ . This statistical precision is enabled by data for a large and homogeneous sample of recently discovered gravitational-lens galaxies. Similar analyses have been carried out previously, but with much lower statistical significance. Nottale [7] applied this type of test to the lensing galaxy cluster A370 to obtain  $0.87 < \gamma < 1.55$ , subject to assumptions about the mass structure of the cluster. Dar [8] found agreement within  $\leq 30\%$  error bars between the observed and predicted image separations in a heterogeneous sample of 5 gravitational-lens systems, also for fixed mass-structure assumptions, but did not translate this result into a constraint on  $\gamma$ . Sirousse-Zia [9] developed formalism for the test, expressing the dependence upon  $\gamma$  of the lensing properties of the singular isothermal sphere galaxy model (see below), but did not derive any observational results.

The dependence of gravitational lensing upon  $\gamma$  can be derived from a general form of the metric for a point mass  $m$  in the weak-field limit for a space-time that yields Newtonian gravity:

$$d\tau^2 = dt^2 \left( 1 - \frac{2m}{r} \right) - dr^2 \left( 1 + \frac{2\gamma m}{r} \right) - r^2 d\phi^2. \quad (1)$$

The parameter  $\gamma$  equals unity for the Schwarzschild metric,  $\phi$  is the angle in the invariant orbital plane, and  $G$  and  $c$  have been set equal to 1. In this formulation, the weak-field gravitational acceleration can be calculated, and is verified to be  $-Gm/r^2$  as given by Newton and independent of the parameter  $\gamma$ . From the speed of light in the radial direction as inferred by an external observer at infinity, one may define an effective index of refraction for the space surrounding the point mass, and hence around any arbitrary

\*Electronic address: [abolton@cfa.harvard.edu](mailto:abolton@cfa.harvard.edu)

mass distribution through the principle of superposition. This quantity is used to compute the Shapiro delay, and for sufficiently isolated gravitational-lens systems one may invoke the thin-lens approximation. Thus gravitational lensing can be formulated in terms of two-dimensional Fermat time delay surfaces [10,11]. By extremizing the sum of the Shapiro and geometric time delays, one obtains the “lens equation” that relates position in the observed image plane to location in the unobserved and unlensed source plane:

$$\vec{\theta}_s = \vec{\theta} - \frac{(1 + \gamma)}{2} \vec{\nabla} \psi(\vec{\theta}). \quad (2)$$

Here,  $\vec{\theta}_s$  is the angular source location,  $\vec{\theta}$  is the angular location of the image, and  $\psi(\vec{\theta})$  is a scaled line-of-sight integral of the Newtonian gravitational potential of the lensing object (see Eq. 48 of [12] for the explicit definition of  $\psi$  in this context). The Einstein radius, defined by  $\vec{\theta}_s = 0$  for circularly-symmetric projected potentials, simply scales with the factor  $(1 + \gamma)/2$ . The difficulty in inferring anything about the  $\gamma$  parameter is that it appears only as a product with the relevant masses of the problem. Unless one knows the lensing mass via some method other than lensing, there is no distinction between, e.g., the solution for a lensing mass  $M$  and  $\gamma = 1$  and the solution for a lensing mass of  $2M$  and  $\gamma = 0$ .

The actual observational test that we perform here can be understood most simply in terms of the singular isothermal sphere (SIS) galaxy model, though we in fact allow for more general galaxy models in our analysis. The SIS is a dynamically self-consistent, spherically-symmetric three-dimensional profile with density  $\rho(r) = \sigma_v^2/(2\pi Gr^2)$ . It is perhaps the best one-parameter model for elliptical galaxies, characterized by an isotropic and radially constant dispersion of stellar orbital velocities  $\sigma_v$  that determines the mass within any given radius. Through gravitational lensing, the SIS forms a ring image of any background objects along the same line of sight, with an angular Einstein radius of

$$\theta_E = (1 + \gamma)2\pi(\sigma_v^2/c^2)(D_{LS}/D_S), \quad (3)$$

where  $D_{LS}$  and  $D_S$  are distance measures discussed further below. Thus, within the context of the SIS model, measurements of the Einstein radii *and* velocity dispersions of gravitational-lens galaxies can be used to constrain the  $\gamma$  parameter [9]. (From an observational standpoint, velocity dispersion is defined in this work as the luminosity-weighted integral of the second moment of the stellar velocity distribution along the observational line of sight. It may be measured from the spectrum of a galaxy whose stellar population is spatially unresolved by fitting for the broadening of stellar atomic absorption lines that best reproduces the features seen in the integrated galaxy spectrum.)

Spatially resolved, high signal-to-noise observations of the kinematics of elliptical galaxies, whose stellar populations are dynamically “hot” (i.e., not characterized by ordered circular orbits), can be used in combination with detailed modeling to deduce radial density profiles and to directly test the validity of the isothermal approximation. Such studies (e.g. [13–19]) indicate a modest amount of dark matter within one half-light radius and an approximately isothermal density profile in elliptical galaxies that are nearby enough to permit the necessary observations. Gravitational-lens galaxies (hereafter GLGs), by contrast, are typically elliptical galaxies at relatively high redshift and with significant contamination from the light of lensed quasar images, and thus do not allow the same type of dynamical analysis as local ellipticals. Thus lensing itself is usually the only robust measurement of the mass of the GLG, and a model for the density profile must simply be assumed. An exception is the Lenses Structure and Dynamics [LSD] Survey [20–24], which has used lens-galaxy velocity dispersions in combination with Einstein radii and the implicit GR assumption of  $\gamma = 1$  to place constraints on the relative contributions of luminous and dark matter in distant GLGs.

The current work is enabled by the significant new sample of relatively low redshift ( $0.06 < z < 0.33$ ) elliptical GLGs presented by the Sloan Lens ACS (SLACS) Survey [25–27]. The SLACS GLGs, which were discovered within the Sloan Digital Sky Survey spectroscopic database (SDSS: [28]), are particularly distinguished by the ease and accuracy with which their surface-brightness profiles and stellar dynamics can be measured, relative to previously known GLGs. Publicly available SDSS velocity-dispersion measurements of SLACS GLGs provide a single, lensing-independent dynamical mass scale for each system, though they do not allow a lensing-independent determination of the GLG density profiles. In this work we adopt the hypothesis that, by virtue of their relatively low redshifts, SLACS GLGs are sufficiently like nearby elliptical galaxies for their *distribution* in density profiles to be approximated by the distribution deduced for nearby elliptical galaxies from the application of detailed dynamical modeling. The masses of SLACS GLGs can thus be inferred independently of lensing from their SDSS velocity dispersions, with an uncertainty quantified by both measurement error and intrinsic scatter in density profile (and velocity anisotropy, discussed below). The most significant evolution to be expected between nearby elliptical galaxies and the SLACS GLGs is in luminosity, which we circumvent by working entirely with mass, shape, and dynamical observables.

In order to work with directly observable quantities (of which galaxy mass is not one), we frame our analysis in terms of a comparison between the stellar velocity dispersions of GLGs (i) as observed and (ii) as predicted from their lensing Einstein radii for a given value of  $\gamma$ . Before

proceeding into more detail, we note that the observed stellar dispersions of SLACS GLGs agree within observational errors with their Einstein radii when the latter are directly translated into velocity dispersions using Eq. (3) and assuming  $\gamma = 1$  (see Fig. 5 of [26]). To incorporate the possible effects of nonisothermal lens profiles, we employ the self-similar, axisymmetric model described by Koopmans [29]. This model approximates the mass- and luminosity-density profiles of GLGs with power-law forms: i.e. three-dimensional mass density  $\rho(r) \propto r^{-\alpha}$  and luminosity density  $\nu(r) \propto r^{-\delta}$  (here we have used  $\alpha$  to replace the  $\gamma'$  of [29] to avoid confusion with the post-Newtonian parameter of interest). With  $\alpha$  and  $\delta$  considered as separate parameters, the model corresponds to a scale-free galaxy with a constant logarithmic radial mass-to-light ratio gradient, capable of describing an increasing dark-matter fraction at increasing radius. Larger values of  $\alpha$  and  $\delta$  correspond to more centrally concentrated mass and light profiles. The observed angular Einstein radius  $\theta_E$  of a GLG gives a measurement of the enclosed mass. Taking the mass normalization set by  $\theta_E$  and fixed values for  $\alpha$  and  $\delta$ , the spherically-symmetric steady-state Jeans equation is integrated analytically for velocity dispersion in the radial direction as a function of radius. (The Jeans equation is obtained from the velocity moments of the collisionless Boltzmann equation for the phase space distribution of stellar orbits in Newtonian gravity; see, e.g., [30]) The model further assumes a constant radial profile for the conventionally defined velocity anisotropy parameter  $\beta$  which relates velocity dispersions in the radial and tangential directions:  $\beta = 1 - \sigma_{v,\text{tan}}^2 / \sigma_{v,\text{rad}}^2$ . The Jeans-equation solution assumes the validity of Newtonian gravitation on the relevant scales, but is independent of  $\gamma$  in the weak-field limit as discussed above. The luminosity-weighted squared velocity dispersion is integrated along the line of sight to give an analytic prediction for the observed velocity dispersion as a function of position within the image of the GLG. The simplest SIS model is described by the special case of  $\alpha = \delta = 2$  and  $\beta = 0$ .

The sample we analyze consists of the 15 SLACS GLGs with published Einstein radii, determined by fitting singular isothermal ellipsoid (SIE) lens models with the normalization of [31] to Hubble Space Telescope (HST) imaging data [27]. Though the SIE model assumes a particular radial mass profile, measured Einstein radii depend only weakly upon the details of the radial mass distribution of the GLG. We obtain  $\delta$  values by computing average logarithmic surface-brightness profile slopes for the 15 systems through nonlinear least-squares fitting of elliptical power-law luminosity models convolved with the instrumental point-spread function to the HST imaging data within a radius of 1.8 arcseconds about the center of each GLG. (A three-dimensional brightness profile  $\nu(r) \propto r^{-\delta}$  will have a projected two-dimensional profile  $I(R) \propto R^{-\delta+1}$ .) Both the mass and light models fitted to the HST data include a

projected minor-to-major axis-ratio parameter  $q$  to allow for ellipticity. To connect these models to the axisymmetric approximation of the analytic Jeans equation-based framework, we use the interchange

$$R \leftrightarrow R_q = \sqrt{qx^2 + y^2/q}, \quad (4)$$

which conserves the total mass or light within a given isodensity or isobrightness contour. Stellar velocity-dispersion values for each GLG are taken from the output of the Princeton 1d spectroscopic pipeline analysis of the SDSS database [32]. The SDSS spectrograph integrates all atmospherically blurred galaxy light within a circular optical-fiber aperture of radius 1.5 arcseconds on the sky. The fractional systematic velocity-dispersion inaccuracy incurred in a circularly-symmetric Jeans analysis of an oblate galaxy is calculated by [33] to be small provided that one uses angularly-averaged velocity dispersions and Einstein radii, as we do in our calculations here. We add this error in quadrature to the observational velocity-dispersion error estimates for each lens, though it is small (median contribution of 2%) and has a negligible effect on our result.

To determine suitable probability distributions for the mass concentration  $\alpha$  and velocity anisotropy  $\beta$  of the SLACS GLGs, we make use of the results of Gerhard *et al.* [15], who compute the density structure for a sample of nearby elliptical galaxies using dynamical observations. From Fig. 1 of that work, we determine the change in circular velocity (or, equivalently, mass enclosed) between 0.2 and 0.6 half-light radii for each of the 17 galaxies with data over that range. The chosen radial range corresponds roughly to the range probed by the SLACS GLG sample. We assign to each of these galaxies a logarithmic radial density slope  $\alpha$  that will give the same relative change in circular velocity. This gives a sample mean log-slope of  $\langle \alpha \rangle = 1.93$  and an intrinsic RMS variation of  $\sigma_\alpha = 0.08$ . From Fig. 5 of the same work, we calculate the average and RMS variation of the velocity anisotropy parameter  $\beta$  to be  $\langle \beta \rangle = 0.18$  and  $\sigma_\beta = 0.13$  (excluding the outlier galaxies NGC 4636 and NGC 4486B). We model the probability distributions of  $\alpha$  and  $\beta$  for the SLACS GLGs as uncorrelated Gaussians with these parameters. Neither of these properties exhibit significant correlation with galaxy mass in [15].

For comparison with the observed velocity dispersions, we integrate the position-dependent velocity dispersion predicted by lensing over the SDSS spectroscopic optical-fiber aperture. The combined effect of the circular SDSS aperture (radius 1.5 arcseconds) and the typical image quality of FWHM 2 arcseconds (due to atmospheric blurring) is well approximated by a circular Gaussian weighted aperture with a FWHM of 2.8 arcseconds, which we combine with luminosity weighting in an integration of Eq. 2.4 of [29]. We furthermore incorporate the dependence of gravitational lensing upon  $\gamma$  and eliminate the

explicit dependence on the mass of the GLG in favor of the Einstein radius to obtain

$$\begin{aligned} \langle \sigma_{\text{l.o.s.}}^2 \rangle &= \frac{c^2}{4\pi} \frac{D_S}{D_{LS}} \theta_E \left( \frac{2}{1+\gamma} \right) f(\alpha, \delta, \beta) \\ &\times \left( \frac{\theta_A}{\theta_E} \right)^{2-\alpha} 2^{1-\alpha/2} \left( \frac{5-\delta-\alpha}{3-\delta} \right) \\ &\times \left( \frac{\Gamma[(5-\delta-\alpha)/2]}{\Gamma[(3-\delta)/2]} \right). \end{aligned} \quad (5)$$

Here, the first occurrence of  $\theta_E$  is to be expressed in radians. The dimensionless function  $f(\alpha, \delta, \beta)$  is given in [29]. The quantity  $\theta_A$  is the ‘‘Gaussian sigma’’ of the spatial weighting aperture: i.e., 2.8 arcseconds divided by 2.355. Additional factors on the second and third lines arise from our use of a Gaussian integration aperture.  $D_S$  and  $D_{LS}$  are angular-diameter distances from the observer to the lensed galaxy and from the GLG to the lensed galaxy, respectively, specifying the angle subtended by a given physical distance transverse to the line of sight. These distances are functions of the redshifts of the two galaxies, which have been measured to high accuracy for all SLACS systems using SDSS spectroscopic data [25].  $D_S$  and  $D_{LS}$  also depend upon the adopted cosmology, and in principle would be altered through the Robertson-Walker metric by any change in  $\gamma$  (as noted by [9]). However, such changes would necessarily be accompanied by changes in the matter-energy density of the universe in order to reproduce the shape of the luminosity distance-redshift relation empirically constrained by type Ia supernova observations out to redshift  $z \approx 1$  [34–37]. Thus although we shall compute  $D_S$  and  $D_{LS}$  under the assumption of the currently favored cosmology with density parameters  $(\Omega_M, \Omega_\Lambda) = (0.3, 0.7)$  [38], we regard this recipe as a suitable proxy for the empirical distance-redshift relation.

We use Eq. (5) to determine numerically the probability distribution of the ‘‘true’’ aperture velocity dispersion  $\langle \sigma_{\text{l.o.s.}}^2 \rangle^{1/2}$ , which we denote below by  $\sigma$  for convenience, for each GLG as a function of  $\gamma$ . This is done by computing  $\sigma$  over a grid of all physically allowed  $\alpha$  and  $\beta$  values (i.e., those that give finite central mass and predict non-negative  $\sigma^2$ ) at fixed  $(\delta, \theta_E, \theta_A)$ , assigning differential weights over the grid as given by the assumed probabilities of  $\alpha$  and  $\beta$ , and sorting in  $\sigma$  to determine the cumulative probability distribution. This computation is repeated over a grid of  $\gamma$  values from 0–4 to derive the desired probability density  $P_1(\sigma|\gamma)$  for each lens. The probability density for obtaining a particular *measured* SDSS velocity dispersion  $\sigma_{\text{SDSS}}$  at fixed  $\gamma$  is then given by

$$P_3(\sigma_{\text{SDSS}}|\gamma) = \int d\sigma P_2(\sigma_{\text{SDSS}}|\sigma) P_1(\sigma|\gamma). \quad (6)$$

For  $P_2(\sigma_{\text{SDSS}}|\sigma)$ , we assume a Gaussian distribution about the true value, with a width given by the measurement error for each system. Statistical errors on the measured  $\delta$  and

$\theta_E$  values are neglected, since they have an exceedingly small effect compared to the errors on the  $\sigma_{\text{SDSS}}$  values and the assumed intrinsic variation in  $\alpha$  and  $\beta$ .

For each GLG  $i$ , given its measured  $\sigma_{\text{SDSS}}$ , Eq. (6) may be interpreted as a likelihood distribution for the parameter  $\gamma$ . Since we expect the true value of  $\gamma$  to be universal and thus the same for all GLGs in the sample, we can express its likelihood distribution given all the data and the prior assumptions as

$$\mathcal{L}(\gamma) = \prod_{\text{lenses } i} P_3^{(i)}(\sigma_{\text{SDSS}}^i|\gamma). \quad (7)$$

Figure 1 shows the individual factors in this likelihood product, as well as the joint normalized likelihood density. Though the distribution of individual maximum-likelihood values seen in Fig. 1 appears slightly bimodal between  $\gamma$  values greater than 1 and less than 1, this effect is not statistically significant: a Kolmogorov-Smirnov test of the distribution of individual  $\gamma$  values indicates a reasonable 33% probability of being drawn from a Gaussian distribution about  $\gamma = 1$  with a width equal to the mean RMS width of the individual  $\gamma$  distributions (approximately 0.3). Furthermore, the individual  $\gamma$  values are not significantly correlated with any lens-galaxy observables. The joint distribution  $\mathcal{L}(\gamma)$  is described well by a Gaussian in  $\gamma$ , from which we derive a maximum-likelihood constraint of  $\gamma = 0.98 \pm 0.07$  (68% confidence).

Our maximum-likelihood value for  $\gamma$  is in excellent agreement with the GR-predicted value of  $\gamma = 1$ . This result is an important quantitative test of the theory of gravitation on scales much larger than have been probed previously with solar-system experiments. The current analysis is enabled by the new sample of GLGs from the SLACS Survey for which lens masses can (implicitly) be estimated through a combination of observables and rea-

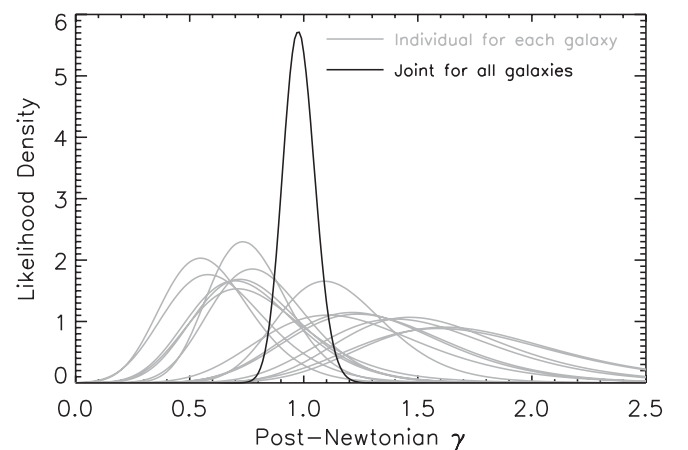


FIG. 1. Normalized likelihood densities for the post-Newtonian parameter  $\gamma$  derived from individual SLACS GLGs (gray), with joint likelihood for the entire sample (black). The joint distribution is approximately Gaussian, giving  $\gamma = 0.98 \pm 0.07$  (68% confidence).

sonable assumptions independent of lensing itself. We note that a spatially resolved and/or higher signal-to-noise observational determination of the stellar dynamics of the SLACS GLGs would remove some of the reliance on prior assumptions based on the local universe, thus making the result more robust.

The authors thank Scott Hughes for valuable feedback about the manuscript. A. S. B. thanks Margaret Geller and Virginia Trimble for questions that first provoked his thoughts on this subject. S. R. acknowledges support from NASA Chandra Grant No. NAG5-TM5-6003X. S. B. acknowledges support from NSF Grant No. AST-0307705. Based on observations made with the NASA/ESA Hubble

Space Telescope, obtained from the Data Archive at the Space Telescope Science Institute, which is operated by AURA, Inc., under NASA contract NAS 5-26555. These observations are associated with program #10174 (PI: L.V.E. Koopmans). Funding for the SDSS and SDSS-II has been provided by the Alfred P. Sloan Foundation, the Participating Institutions, the National Science Foundation, the U.S. Department of Energy, NASA, the Japanese Monbukagakusho, the Max Planck Society, and the Higher Education Funding Council for England. The SDSS Web Site is <http://www.sdss.org/>. The SDSS is managed by the Astrophysical Research Consortium for the Participating Institutions.

- 
- [1] F. Zwicky, *Phys. Rev.* **51**, 290 (1937).
- [2] B. Bertotti, L. Iess, and P. Tortora, *Nature (London)* **425**, 374 (2003).
- [3] J. M. Weisberg and J. H. Taylor, *Phys. Rev. Lett.* **52**, 1348 (1984).
- [4] C. M. Will and K. J. Nordtvedt, *Astrophys. J.* **177**, 757 (1972).
- [5] C. W. Misner, K. S. Thorne, and J. A. Wheeler, *Gravitation* (W. H. Freeman and Co., San Francisco, 1973).
- [6] I. I. Shapiro, *Phys. Rev. Lett.* **13**, 789 (1964).
- [7] L. Nottale, in *Dark matter; Proceedings of the Twenty-third Rencontre de Moriond (Eighth Moriond Astrophysics Workshop), Les Arcs, France, 1988 (A90-12876 02-90)*, edited by J. Audouze and J. Tran Thanh Van (Gif-sur-Yvette, France, Editions Frontieres, 1988), pp. 339–346.
- [8] A. Dar, *Nucl. Phys. B, Proc. Suppl.* **28**, 321 (1992).
- [9] H. Sirousse-Zia, *Gen. Relativ. Gravit.* **30**, 1273 (1998).
- [10] P. Schneider, *Astron. Astrophys.* **143**, 413 (1985).
- [11] R. Blandford and R. Narayan, *Astrophys. J.* **310**, 568 (1986).
- [12] R. Narayan and M. Bartelmann, astro-ph/9606001.
- [13] R. P. van der Marel, *Mon. Not. R. Astron. Soc.* **253**, 710 (1991).
- [14] A. Kronawitter, R. P. Saglia, O. Gerhard, and R. Bender, *Astron. Astrophys. Suppl. Ser.* **144**, 53 (2000).
- [15] O. Gerhard, A. Kronawitter, R. P. Saglia, and R. Bender, *Astron. J.* **121**, 1936 (2001).
- [16] A. J. Romanowsky and C. S. Kochanek, *Astrophys. J.* **553**, 722 (2001).
- [17] E. Emsellem *et al.*, *Mon. Not. Roy. Astron. Soc.* **352**, 721 (2004).
- [18] M. Cappellari *et al.*, *Mon. Not. Roy. Astron. Soc.* **366**, 1126 (2006).
- [19] R. P. van der Marel and M. Franx, *Astrophys. J.* **407**, 525 (1993).
- [20] L. V. E. Koopmans and T. Treu, *Astrophys. J. Lett.* **568**, L5 (2002).
- [21] L. V. E. Koopmans and T. Treu, *Astrophys. J.* **583**, 606 (2003).
- [22] T. Treu and L. V. E. Koopmans, *Astrophys. J.* **575**, 87 (2002).
- [23] T. Treu and L. V. E. Koopmans, *Mon. Not. Roy. Astron. Soc.* **343**, L29 (2003).
- [24] T. Treu and L. V. E. Koopmans, *Astrophys. J.* **611**, 739 (2004).
- [25] A. S. Bolton, S. Burles, L. V. E. Koopmans, T. Treu, and L. A. Moustakas, *Astrophys. J.* **638**, 703 (2006).
- [26] T. Treu, L. V. E. Koopmans, A. S. Bolton, S. Burles, and L. A. Moustakas, *Astrophys. J.* **640**, 662 (2006).
- [27] L. V. E. Koopmans, T. Treu, A. S. Bolton, S. Burles, and L. A. Moustakas, *Astrophys. J.* (to be published).
- [28] D. G. York *et al.*, *Astron. J.* **120**, 1579 (2000).
- [29] L. V. E. Koopmans, in *Proceedings of XXIst IAP Colloquium*, edited by G. A. Mamon, F. Combes, C. Deffayet, and B. Fort (EDP Sciences, Paris, 2006), pp. 161–166.
- [30] J. Binney and S. Tremaine, *Galactic Dynamics* (Princeton University Press, Princeton, NJ, 1987), p. 747.
- [31] R. Kormann, P. Schneider, and M. Bartelmann, *Astron. Astrophys.* **284**, 285 (1994).
- [32] <http://spectro.princeton.edu>.
- [33] C. S. Kochanek, *Astrophys. J.* **436**, 56 (1994).
- [34] A. G. Riess *et al.*, *Astron. J.* **116**, 1009 (1998).
- [35] S. Perlmutter *et al.*, *Astrophys. J.* **517**, 565 (1999).
- [36] R. A. Knop *et al.*, *Astrophys. J.* **598**, 102 (2003).
- [37] A. G. Riess *et al.*, *Astrophys. J.* **607**, 665 (2004).
- [38] D. N. Spergel *et al.*, *Astrophys. J. Suppl. Ser.* **148**, 175 (2003).